# Slow-Down vs. Speed-Up of Information Diffusion in Non-Markovian Temporal Networks

**Ingo Scholtes, Nicolas Wider, René Pfitzner, Antonios Garas, Claudio Juan Tessone and Frank Schweitzer**
Chair of Systems Design, ETH Zurich, Switzerland
`www.sg.ethz.ch`

**Abstract**

We study the slow-down and speed-up of information diffusion in temporal networks with non-Markovian contact sequences. We introduce a causality-preserving time-aggregated representation that allows to analyze temporal networks from the perspective of spectral graph theory. With this we provide the first analytical explanation for the frequently observed slow-down of information diffusion in empirical non-Markovian temporal networks. We derive an analytical prediction for the magnitude of this slow-down and validate our prediction against two empirical data sets. Counterintuitively, we further show that non-Markovian properties can result in a speed-up of information diffusion that can be related to the spectral properties of the underlying temporal network.

The evolution of dynamical processes in temporal networks can deviate significantly from what one would expect from their corresponding static, time-aggregated representations. Non-Markovian properties in the contact sequences of temporal networks have been identified as one important mechanism which (i) alters the topology of causal interactions and (ii) can significantly change the dynamics of diffusion processes in real-world temporal networks [1, 2, 3, 4]. So far, an analytical explanation for the differences that are due to these correlations, as well as for the significant variations observed across different real-world systems is missing. To fill this gap, in this Letter we introduce an analytical approach that allows to study Laplacian dynamics in temporal networks with non-Markovian contact sequences. In particular, (i) we introduce higher-order time-aggregated representations of temporal networks that preserve causality, (ii) we define statistical ensembles of temporal networks with fixed aggregate topologies and statistics of time-respecting paths, (iii) we show that spectral properties of higher-order aggregate networks provide an explanation for changes of random walk convergence in temporal networks compared to aggregate networks, and (iv) we derive an analytical estimation for the direction and magnitude of the change expected in a particular temporal network that is validated by empirical data.

We define a temporal network as a tuple $G^T = (V, E^T)$ consisting of nodes $V$ and a set of directed, time-stamped edges $(a, b; t) \in E^T$ for $a, b \in V$. We further assume a discrete notion of time $t \in \{0, \dots, L\}$ where $L$ is the length of the observation period. Based on a temporal network $G^T$, a (first-order) time-aggregated representation can be defined as $G^{(1)} = \left(V, E^{(1)}\right)$

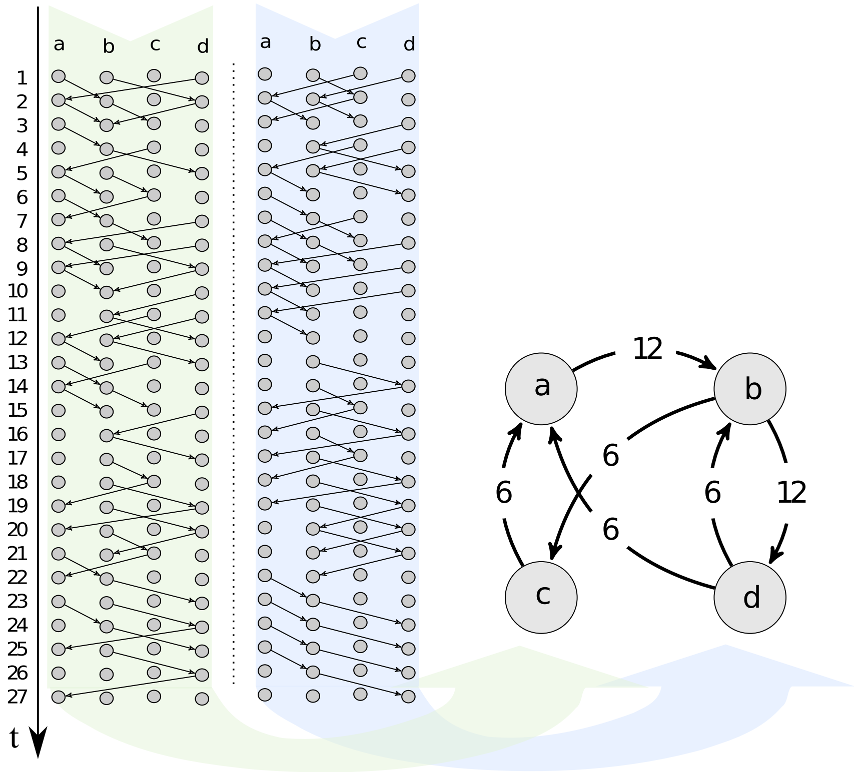

Figure 1: Two different temporal networks $G^T$ (left) and $\hat{G}^T$ (right) giving rise to the same weighted, time-aggregated network $G^{(1)}$

with $E^{(1)} \subseteq V \times V$ and $(a, b) \in E^{(1)}$ iff $\exists t \in \{0, \ldots, L\}$ such that $(a, b; t) \in E^T$. A weight function $w^1 : E^{(1)} \to \mathbb{R}$ can then be defined as the (relative) number of edge occurrences. A simple way to illustrate temporal networks are *time-unfolded* representations, in which time is unfolded into an additional topological dimension. In the resulting time-unfolded representation nodes $v \in V$ are replaced by temporal copies $v_t$ for each time step $t$, while time-stamped edges $(v, w; t)$ are represented by edges $(v_t, w_{t+1})$. Time-unfolded representations of two different temporal networks $G^T$ and $\hat{G}^T$ that result in the same weighted aggregated network $G^{(1)}$ are shown in Fig. 1.

An important characteristic of temporal networks is that, compared to their corresponding time-aggregated representations, the transitivity of paths does not necessarily hold. In particular, a *path* $(a, b) \to (b, c)$ in a time-aggregated network does not imply that $a$ and $c$ are connected via a *time-respecting path* in the temporal network. A time-respecting path connecting $a$ and $c$ only exists if the edge $(a, b; t)$ occurs *before* $(b, c; t')$, i.e. $t < t'$. Hence, the order of interactions in temporal networks significantly affects the topology of time-respecting paths - and thus causality

- in dynamic complex systems.

A particularly simple way to study causality in temporal networks is in terms of the statistics of time-respecting paths of length two, so-called *two-paths* consisting of two edges $(a, b) \to (b, c)$. Recent studies revealed that - compared to what one expects from a weighted time-aggregated network - nodes often preferentially mediate information flows between particular pairs of their neighbors. Thus, such temporal networks have non-Markovian characteristics, since the next contact in a contact sequence depends not only on the current, but also on the previous one. This characteristic has been shown to be present in a number of real-world systems and it has been proven to be responsible for significant changes in diffusion dynamics [1, 2, 3]. To illustrate this effect, we compute the total variation distance ($\Delta$), as a measure of convergence of a random walk process, for three empirical temporal networks: (AN) social interactions in ant colonies [5]; (RM) time-stamped social interactions between students and academic staff members at a university [6]; and (SN) a synthetic contact sequence for which the aggregate network shows two pronounced communities and in which non-Markovian properties enforce two-paths across communities. We define the total variation distance between two probability distributions $\mu$ and $\pi$ as $\Delta(\mu, \pi) := \frac{1}{2} \sum_x |\pi(x) - \mu(x)|$. Fig. 2 shows the slow-down $\mathcal{S}(\Delta) := t_{temp}(\Delta)/t_{agg}(\Delta)$ based on the average times $t_{agg}(\Delta)$ and $t_{temp}(\Delta)$ after which total variation distance of a random walk falls below a given $\Delta$ in (i) the static, time-aggregated network and (ii) a temporal network model derived from the empirical contact sequence respectively. In order to focus on non-Markovian properties and exclude the effect of inter-event time distributions, the temporal network model preserves only the distribution of two-paths in the contact sequence as well as the weighted aggregate network. For the three temporal networks one finds that - even though they are of comparable size[1] - the deviations from the dynamics in the corresponding aggregate networks are very different. For (RM) we obtain a maximum slow-down of $\mathcal{S} \approx 8.8 \pm 0.3$, while for (AN) the maximum slow-down is $\mathcal{S} \approx 1.8 \pm 0.1$. For (SN), the deviation peaks at $\mathcal{S} \approx 0.86 \pm 0.1$, hence indicating a significant speed-up of convergence compared to the aggregate network.

In the following we provide an analytical explanation for the direction of this change (i.e. slow-down or speed-up) as well as for its magnitude in a particular temporal network. In particular, we show that spectral properties of a higher-order, time-aggregated network allow to calculate an analytical estimate $\mathcal{S}^*$ for the slow-down factor $\mathcal{S}$ observed in empirical temporal networks. Assuming only three-point correlations, non-Markovian characteristics in the *sequence of nodes* can be eliminated by considering instead a stochastic process that generates a *sequence of edges*. By this state space extension of the underlying stochastic process one can obtain a Markovian representation of temporal networks in which nodes exhibit a "one-step memory" in terms of determining the next interaction. For this, we define a *second-order* time-aggregated network $G^{(2)} = (V^{(2)}, E^{(2)})$ with $V^{(2)} = E^{(1)}$, i.e. each node $e \in V^{(2)}$ in the network $G^{(2)}$ represents an

[1] The networks consist of 61 (AN), 58 (RM), and 100 (SN) nodes.

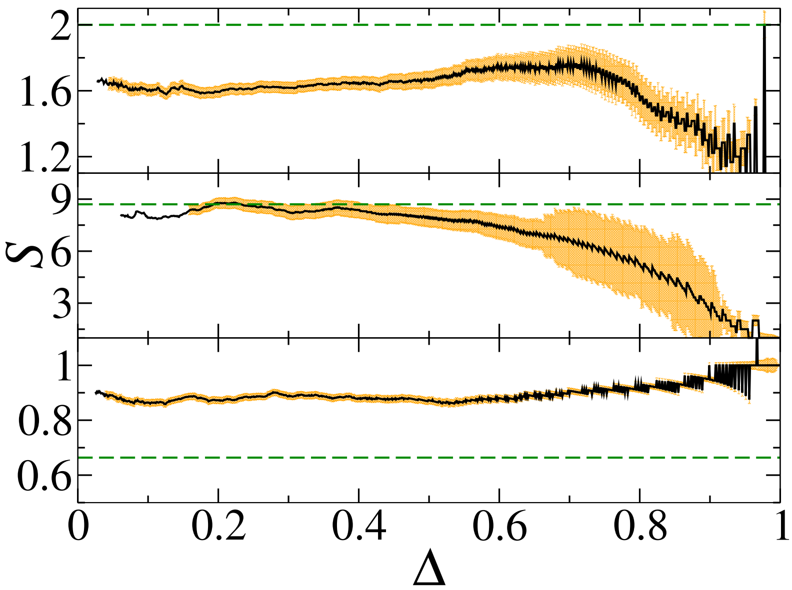


Figure 2: Slowdown factor ($\mathcal{S}$) of random walk convergence in temporal networks generated by (i) a model preserving two-path statistics compared to (ii) a random walk in the weighted time-aggregated network for the (AN) (top), (RM) (middle) and (SN) dataset (bottom). Results are averages of 1000 realizations, error bars indicate the standard error. The predicted $\mathcal{S}^*$ value (see Eq. 9) is shown by the horizontal dashed line.

edge $e \in E^{(1)}$ in the time-aggregated network $G^{(1)}$. As edges $(e_1, e_2) \in E^{(2)} \subseteq E^{(1)} \times E^{(1)}$, we define all possible paths of length two in the aggregate network $G^{(1)}$, i.e.

$$E^{(2)} := \left\{ (e_1, e_2) \, | e_1 = (a, b), e_2 = (b, c) \in E^{(1)} \right\}.$$

Based on a temporal network $G^T$, a weight function $w^{(2)} : E^{(2)} \to \mathbb{R}$ can be defined as the frequency of paths $(e_1, e_2) = (a, b) \to (b, c)$ while proportionally correcting the weights of multiple two-paths $(a', b) \to (b, c')$ passing through the same node $b$. For $e_1 = (a, b)$ and $e_2 = (b, c)$ we thus define [2]

$$w^{(2)}(e_1, e_2) := \sum_{t=1}^{L} \frac{\delta_{(a,b;t-1)}\delta_{(b,c;t)}}{\sum_{a',c' \in V} \delta_{(a',b;t-1)}\delta_{(b,c';t)}}, \tag{1}$$

where $\delta_x = \delta_x(E^T)$ is an indicator function, i.e.

$$\delta_{(e;t)}\left(E^T\right) = \begin{cases} 1 \text{ iff } (e;t) \in E^T \\ 0 \text{ otherwise.} \end{cases}$$

[2]It is simple to generalize this weight function to capture two-paths $(a, b; t') - (b, c, t)$ for $1 \leq t - t' \leq \epsilon$

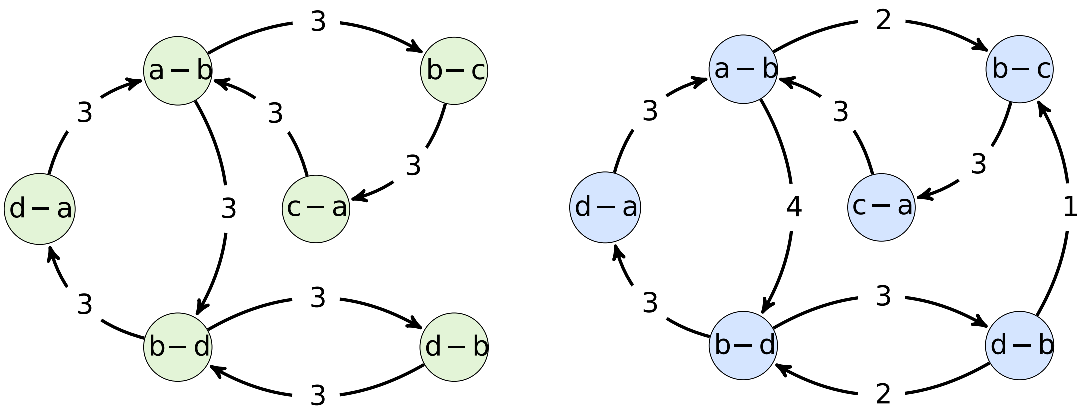


Figure 3: Two second-order time-aggregated representations $G^{(2)}$ (left) and $\hat{G}^{(2)}$ (right) corresponding to the two temporal networks $G^T$ and $\hat{G}^T$ shown in Fig. 1. Both second-order time-aggregated networks are consistent with $G^{(1)}$ depicted in Fig. 1.

By this construction we obtain a *second-order time-aggregated network* $G^{(2)}$ in which (i) each node $e \in V^{(2)}$ represents an edge in the underlying temporal network $G^T$, (ii) each edge $(e_1, e_2)$ represents a time-respecting path of length two, and (c) the weights $w^{(2)} : E^{(2)} \to \mathbb{R}$ capture the statistics of two-paths in $G^T$. Two second-order time-aggregated networks $G^{(2)}$ and $\hat{G}^{(2)}$ with weights corresponding to the two example networks $G^T$ and $\hat{G}^T$ in Fig. 1 are depicted in Fig. 3. Using the weights $w^{(2)}$, for $e_1, e_2 \in V^{(2)}$ we define the entries $T^{(2)}_{e_1,e_2}$ of a row stochastic matrix $\mathbf{T}^{(2)}$ as

$$T^{(2)}_{e_1 e_2} := w^{(2)}\left(e_1, e_2\right) \left( \sum_{e' \in V^{(2)}} w^{(2)}\left(e_1, e'\right) \right)^{-1}. \tag{2}$$

It is easy to see that - if $\mathbf{T}^{(2)}$ is irreducible, aperiodic and reversible - the resulting unique (normalized) Perron-Frobenius eigenvector $\pi$ of $\mathbf{T}^{(2)}$ gives the stationary activation frequencies of edges. As such, for each $e = (a, b) \in V^2$ the weight $w^{(1)}$ can be defined based on the corresponding element $\pi_e$ of $\pi$ as

$$w^1(a, b) := \pi_e.$$

For the temporal network $G^T$ shown in Fig. 1 (left) and its second-order time-aggregated network $G^{(2)}$ shown in Fig. 3 (left), the corresponding transition matrix $\mathbf{T}^{(2)}$ (with rows/columns ordered as indicated) is given as

$$\mathbf{T}^{(2)} = \begin{array}{c} (a,b) \\ (b,c) \\ (b,d) \\ (c,a) \\ (d,a) \\ (d,b) \end{array} \left| \begin{pmatrix} 0 & 1/2 & 1/2 & 0 & 0 & 0 \\ 0 & 0 & 0 & 1 & 0 & 0 \\ 0 & 0 & 0 & 0 & 1/2 & 1/2 \\ 1 & 0 & 0 & 0 & 0 & 0 \\ 1 & 0 & 0 & 0 & 0 & 0 \\ 0 & 0 & 1 & 0 & 0 & 0 \end{pmatrix} \right. . \tag{3}$$

As Perron-Frobenius eigenvector of $\mathbf{T}^{(2)}$ we obtain $\pi = \left(\frac{1}{4}, \frac{1}{8}, \frac{1}{4}, \frac{1}{8}, \frac{1}{8}, \frac{1}{8}\right)$, thus recovering the relative weights of edges $w^{(1)}$ in the first-order time-aggregated network. Interpreting $\mathbf{T}^{(2)}$ as a transition matrix for a random walker in $G^{(2)}$, we obtain a second-order Markov model that generates contact sequences which preserve (i) the weights in the first-order time-aggregated network, and (ii) the statistics of time-respecting paths of length two and thus the causal topology of the temporal network underlying $G^{(2)}$. From this perspective, the weighted aggregate network $G^{(1)}$ can be seen as a first-order approximation where weights $w^{(1)}(a, b)$ capture the statistics of paths of length one. Contact sequences generated by a random walk in $G^{(1)}$ with transition probabilities proportional to edge weights $w^{(1)}(a, b)$ preserve the statistics of edges but destroy the statistics of two-paths. As such, a random walk in $G^{(1)}$ represents a null model that changes the statistics of time-respecting paths and thus alters causality in temporal networks. The same null model can be defined based on $G^{(2)}$ by constructing a maximum entropy transition matrix $\tilde{\mathbf{T}}^{(2)}$ which (i) preserves the weights $w^{(1)}$ of edges in $G^{(1)}$ and (ii) creates "Markovian" temporal networks. For $e_1 = (a, b)$ and $e_2 = (b, c)$ the entries $\tilde{T}^{(2)}_{e_1 e_2}$ are given as

$$\tilde{T}^{(2)}_{e_1 e_2} := w^{(1)}(b, c) \left( \sum_{c' \in V^{(1)}} w^{(1)}(b, c') \right)^{-1} . \tag{4}$$

For the example aggregate network $G^{(1)}$ depicted in Fig. 1, $\tilde{\mathbf{T}}^{(2)}$ is given as

$$\tilde{\mathbf{T}}^{(2)} = \begin{pmatrix} 0 & 1/3 & 2/3 & 0 & 0 & 0 \\ 0 & 0 & 0 & 1 & 0 & 0 \\ 0 & 0 & 0 & 0 & 1/2 & 1/2 \\ 1 & 0 & 0 & 0 & 0 & 0 \\ 1 & 0 & 0 & 0 & 0 & 0 \\ 0 & 1/3 & 2/3 & 0 & 0 & 0 \end{pmatrix}, \tag{5}$$

where rows and columns are ordered as in Eq. 3.

Each transition matrix $\mathbf{T}^{(2)}$ of a random walk process in $G^{(2)}$ whose Perron-Frobenius eigenvector $\pi$ satisfies $\pi_e = w^{(1)}(e)$ defines a statistical ensemble of temporal networks constrained by a weighted time-aggregated network $G^{(1)}$ and a given statistics of time-respecting paths of length two [3]. Based on the state space $E^{(1)}$ of a random walk in $G^{(2)}$, the ensemble $\Sigma(\mathbf{T}^{(2)})$ of all infinite-length temporal networks generated by a transition matrix $\mathbf{T}^{(2)}$ can be given as

$$\Sigma(\mathbf{T}^{(2)}) := \left\{(e_0, e_1, \ldots) : e_i \in E^{(1)}, T^{(2)}_{e_i e_{i+1}} > 0, i \in \mathbb{N}\right\}.$$

The entropy of such a statistical ensemble can be defined based on the entropy growth rate of the underlying stochastic model $\mathbf{T}^{(2)}$ as

$$H(\mathbf{T}^{(2)}) := - \sum_{e \in E^{(1)}} \pi_e \sum_{e' \in E^{(1)}} T^{(2)}_{ee'} \log_2 \left(T^{(2)}_{ee'}\right). \tag{6}$$

Different from entropy measures that have previously been applied to dynamic networks [7], this entropy quantifies to what extent the next step in a contact sequence is determined by the previous contact and thus considers the causal topology of a temporal network that is due to the order of interactions. For a transition matrix $\mathbf{T}^{(2)}$, the ratio of entropy growth between $\mathbf{T}^{(2)}$ and the (maximum entropy) null model $\tilde{\mathbf{T}}^{(2)}$ can be given as

$$\Lambda_H(\mathbf{T}^{(2)}) := H(\mathbf{T}^{(2)})/H(\tilde{\mathbf{T}}^{(2)}). \tag{7}$$

This ratio ranges between 0 for transition matrices generating deterministic contact sequences and 1 for the maximum entropy case $\tilde{\mathbf{T}}^{(2)}$ representing a Markovian temporal network. For the example in Eq. 3 and the null model given in Eq. 5 we obtain $\Lambda_H(\mathbf{T}^{(2)}) = 0.84$. $\Lambda_H(\mathbf{T}^{(2)}) < 1$ highlights that - for temporal networks in the $\Sigma(\mathbf{T}^{(2)})$ - the statistics of two-paths deviates from what one would expect based on the first-order aggregate network. As such, $\Lambda_H$ provides a simple measure for the importance of non-Markovian properties in a temporal network that indicates whether its causal topology is expected to deviate from the first-order network $G^{(1)}$.

**Information Diffusion in Temporal Networks.** An interesting aspect of representing temporal networks by $G^{(2)}$ is that Laplacian dynamics can be related to spectral properties of the stochastic matrix $\mathbf{T}^{(2)}$. Notably, the same is not true for the first-order representation $G^{(1)}$, since transitivity does not necessarily hold in terms of time-respecting paths; i.e. the existence of edges $(a, b)$ and $(b, c)$ in $E^{(1)}$ does not imply that a time-respecting path connecting $a$ and $c$ exists. However, the existence of edges $(e_1, e_2)$ and $(e_2, e_3)$ in $E^{(2)}$ implies that $(e_1; t_1), (e_2; t_2), (e_3; t_3)$ exist in $E^T$ for time stamps $t_1 < t_2 < t_3$. Hence a time-respecting path $e_1 \to e_2 \to e_3$ exists and transitivity holds in $G^{(2)}$. This allows to relate the spectral properties of $\mathbf{T}^{(2)}$ with Laplacian dynamics in temporal networks with this form of "one-step memory". In particular, the second largest eigenvalue $\lambda_2$ of $\mathbf{T}^{(2)}$ allows to constitute an upper bound for the convergence of (lazy)

[3] Note that this approach can be generalized to $n$-th order networks $G^{(n)}$ and stochastic matrices $\mathbf{T}^{(n)}$ that capture the statistics of time-respecting paths of any length $n$.

random walks with transition matrix $\mathbf{T}^{(2)}$. For a non-complete, directed network $G^{(2)}$ and a stochastic matrix $\mathbf{T}^{(2)}$ with (not necessarily real) eigenvalues $1 = \lambda_1 > |\lambda_2| > \ldots$ a quantity $\mathcal{L}$ can be defined as

$$\mathcal{L}(\mathbf{T}^{(2)}) := 1/\min(1 - |\lambda_2|, 1). \tag{8}$$

The upper bound for the time after which the total variation distance $\Delta(\pi, p)$ between the visitation probabilities $p$ of a random walk and its stationary distribution $\pi$ falls below a threshold $\epsilon$ has been shown to be proportional to this quantity [8]. For a stochastic matrix $\mathbf{T}^{(2)}$ representing an ensemble of temporal networks, we can thus define a slow-down factor as

$$\mathcal{S}^*(\mathbf{T}^{(2)}) := \mathcal{L}(\mathbf{T}^{(2)})/\mathcal{L}(\mathbf{T}^{(1)}), \tag{9}$$

where $\mathbf{T}^{(1)}$ is the transition matrix of a random walk in $G^{(1)}$. For sufficiently large systems, $\mathcal{S}^*(\mathbf{T}^{(2)})$ provides an analytical estimate for (i) the upper bound of the slow-down, and (ii) the lower bound of the speed-up of random walk convergence that is due to non-Markovian properties of a temporal network. Since the null model $\tilde{\mathbf{T}}^{(2)}$ provides an alternative formulation of a random walker in $G^{(1)}$ with transition probabilities proportional to weights $w^{(1)}$, it is easy to see that $\mathcal{L}(\mathbf{T}^{(1)}) = \mathcal{L}(\tilde{\mathbf{T}}^{(2)})$, i.e. $\mathcal{S}(\tilde{\mathbf{T}}^{(2)}) = 1$. For temporal network ensembles defined by $\mathbf{T}^{(2)}$ with $\Lambda_H(\mathbf{T}^{(2)}) < 1$, non-trivial relations between $\mathcal{L}(\mathbf{T}^{(2)})$ and $\mathcal{L}(\mathbf{T}^{(1)})$ can occur which can result both in a slow-down ($\mathcal{S}^*(\mathbf{T}^{(2)}) > 1$), or speed-up ($\mathcal{S}^*(\mathbf{T}^{(2)}) < 1$) of convergence speed.

**Data Analysis.** We now study the effect of non-Markovian characteristics for the empirical temporal networks introduced above. We construct the first-order time-aggregated network $G^{(1)}$ as well as the transition matrices $\mathbf{T}^{(2)}$ and $\tilde{\mathbf{T}}^{(2)}$ as defined in Eqs. 2 and 4. To quantify the importance of non-Markovian characteristics, we first compute the entropy growth rate ratio $\Lambda_H$ for the corresponding statistical ensembles. For (RM) we obtain $\Lambda_H(\mathbf{T}^{(2)}) \approx 0.39$, for (AN) we obtain $\Lambda_H(\mathbf{T}^{(2)}) \approx 0.43$, while for (SN) we obtain $\Lambda_H(\mathbf{T}^{(2)}) \approx 0.24$. This indicates that the topology of time-respecting paths in all three cases is expected to differ significantly from what one would expect based on the first-order aggregate network. The impact of these differences on random walk convergence can be analyzed by calculating $\mathcal{S}^*(\mathbf{T}^{(2)})$. For (RM) we get $\mathcal{S}^*(\mathbf{T}^{(2)}) \approx 8.7$, for (AN) we get $\mathcal{S}^*(\mathbf{T}^{(2)}) \approx 2.0$, while for (SN) we obtain $\mathcal{S}^*(\mathbf{T}^{(2)}) \approx 0.66$. These analytical estimates for the upper bound of the slow-down and the lower bound of the speed-up of random walk convergence are consistent with the changes observed in Fig. 2. In particular, the significantly smaller magnitude of the slow-down in (AN) compared to (RM) can neither be attributed to differences in system size nor inter-event time distributions (which are removed by our model). A spectral analysis of the causality-preserving second-order network allows to explain the smaller slow-down in terms of a “better connected” causal topology of (AN) compared to (RM) that is likely to be related to the larger entropy growth rate in (AN). For (SN) the analytical estimate of $\mathcal{S}^*(\mathbf{T}^{(2)}) \approx 0.66$ is consistent with the speed-up observed in Fig. 2.

Here $\mathcal{S}^*(\mathbf{T}^{(2)}) < 1$ highlights that non-Markovian properties of the contact sequence *mitigate the decelerating effect of community structures* on diffusion dynamics [9] and thus create a causal topology that is "better connected" than what is expected from the aggregate network.

In summary, we introduce second-order aggregate representations of non-Markovian temporal networks. This abstraction allows to define Markov models generating statistical ensembles of temporal networks that preserve (i) the weighted time-aggregated network and (ii) the statistics of time-respecting paths of length two [see Eq. 2]. A transition matrix for this model can easily be computed based on empirical contact sequences. The ratio of entropy growth [see Eq. 7] between this transition matrix and that of a null model generated from the (first-order) aggregate network allows to assess the importance of non-Markovian properties in a particular temporal network. We further show that spectral properties of the transition matrices capture the connectivity of the causal topology of temporal networks and allow to predict (i) whether non-Markovian properties slow down or speed up random walk convergence and (ii) the magnitude of this change [see Eqs. 8 and 9]. Our approach provides the first analytical explanation for previously observed changes in diffusion dynamics in real-world temporal networks with non-Markovian contact sequences.

Finally, we argue that the second-order aggregate networks introduced in this Letter are particularly simple static representations of temporal networks which - in contrast to first-order aggregate networks - preserve causality. We expect further studies of this representation to provide interesting perspectives for (i) the detection of temporal communities by spectral clustering, (ii) refined centrality measures in dynamic networks, and (iii) the analytical study of dynamical processes in complex systems with time-varying interaction topologies.

**Acknowledgements.** We acknowledge feedback by Rebekka Burkholz on the manuscript. N.W., A.G. and F.S. acknowledge support by the EU-FET project MULTIPLEX 317532.

## References

[1] René Pfitzner, Ingo Scholtes, Antonios Garas, Claudio J. Tessone, and Frank Schweitzer. Betweenness preference: Quantifying correlations in the topological dynamics of temporal networks. *Phys. Rev. Lett.*, 110:198701, May 2013.

[2] Hartmut H. K. Lentz, Thomas Selhorst, and Igor M. Sokolov. Unfolding accessibility provides a macroscopic approach to temporal networks. *Phys. Rev. Lett.*, 110:118701, Mar 2013.

[3] M. Rosvall, A. V. Esquivel, A. Lancichinetti, J. D. West, and R. Lambiotte. Networks with Memory. *ArXiv e-prints*, May 2013.

[4] Lauri Kovanen, Kimmo Karsai, János Kertész, and Jari Saramäki. Temporal motifs reveal homophily, gender-specific patterns and group talk in mobile communication networks. *ArXiv e-prints*, pages 1–8, February 2013.

[5] Benjamin Blonder and Anna Dornhaus. Time-ordered networks reveal limitations to information flow in ant colonies. *PLoS ONE*, 6(5):e20298, 05 2011.

[6] Nathan Eagle and Alex (Sandy) Pentland. Reality mining: sensing complex social systems. *Personal Ubiquitous Comput.*, 10(4):255–268, March 2006.

[7] Kun Zhao, Márton Karsai, and Ginestra Bianconi. Entropy of dynamical social networks. *PLoS ONE*, 6(12):e28116, 12 2011.

[8] Fan Chung. Laplacians and the cheeger inequality for directed graphs. *Annals of Combinatorics*, 9:1–19, 2005.

[9] Marcel Salathé and James H. Jones. Dynamics and control of diseases in networks with community structure. *PLoS Comput Biol*, 6(4):e1000736, 04 2010.